Gene Expression, Vol. 18, pp. 135–147
Printed in the USA.

1052-2166/18 $90.00 + .00
DOI: https://doi.org/10.3727/105221618X15174108894682
E-ISSN 1555-3884
www.cognizantcommunication.com

The Effect of Selective c-MET Inhibitor on Hepatocellular Carcinoma in the MET-Active, β-Catenin-Mutated Mouse Model

Na Zhan,*†‡ Adeola Adebayo Michael,*‡ Kaiyuan Wu,† Gang Zeng,* Aaron Bell,*‡ Junyan Tao,*‡ and Satdarshan P. Monga*‡§

*Division of Experimental Pathology, Department of Pathology, University of Pittsburgh School of Medicine, Pittsburgh, PA, USA
†Department of Pathology, Renmin Hospital of Wuhan University, Wuhan, P.R. China
‡Pittsburgh Liver Research Center, University of Pittsburgh Medical Center and University of Pittsburgh School of Medicine, Pittsburgh, PA, USA
§Division of Gastroenterology, Hepatology and Nutrition, Department of Medicine, University of Pittsburgh School of Medicine, Pittsburgh, PA, USA

Simultaneous mutations in CTNNB1 and activation of c-MET occur in 9%–12.5% of patients with hepatocellular carcinoma (HCC). Coexpression of c-MET-V5 and mutant β-catenin-Myc in mouse liver by sleeping beauty transposon/transposase and hydrodynamic tail vein injection (SB-HTVI) led to the development of HCC with 70% molecular identity to the clinical subset. Using this model, we investigated the effect of EMD1214063, a highly selective c-MET inhibitor. Five weeks after SB-HTVI when tumors were established, EMD1214063 (10 mg/kg) was administered by gastric gavage as a single agent on 5-day-on/3-day-off schedule, compared to vehicle only control. Mice were harvested at 8 or 11 weeks posttreatment. Decreased p-MET, p-AKT, p-STAT3, and p-ERK proved in vivo efficacy of EMD1214063. We observed lower Ki-67, PCNA, V5-tag, and cyclin D1 after EMD1214063 treatment only at 8 weeks. Overall, no significant differences were observed in tumor burden between the groups, although EMD1214063 marginally but significantly improved overall survival by 1.5–2 weeks. Tumors remained α-fetoprotein$^+$, did not show any differences in inflammation, and lacked fibrosis in either group. In conclusion, c-MET inhibition alone had a minor effect on Met-β-catenin HCC at the early stages of HCC development. Thus, a single therapy with the c-MET inhibitor will be insufficient for sustained response in Met-β-catenin HCC requiring assessment of additional combinations.

Key words: Hepatocyte growth factor (HGF)/c-MET; β-Catenin; c-MET inhibitor; EMD1214063; Hepatocellular carcinoma (HCC)

INTRODUCTION

Hepatocellular carcinoma (HCC) is a primary malignancy of the liver and is the third most lethal cancer worldwide, with over 500,000 new cases of HCC diagnosed each year[1,2]. Both the incidence rates and death rates due to HCC are increasing in the US and other parts of the world. Analysis of the National Cancer Institute Surveillance, Epidemiology and End Results (SEER) Database of the National Cancer Institute in the US revealed alarming trends in HCC incidence[3,4]. Unfortunately, HCC is typically diagnosed late in its course, with a median survival following diagnosis of approximately 6 to 20 months. In the US, 2-year survival is less than 50%, and 5-year survival is less than 20%[3,4]. Liver transplantation and surgical resection are considered the most effective treatments of HCC. However, surgical treatments are only appropriate for a minority of patients. Other therapeutic options are limited, with only two systemic therapies: first-line sorafenib and second-line regorafenib[5]. Unfortunately, these two drugs extend the median overall survival of patients with advanced HCC by <3 months. Recent accelerated approval of the immunotherapeutic nivolumab underscores the importance of further molecular characterization of HCC for

Address correspondence to Satdarshan P. Monga, M.D., FAASLD, Endowed Chair for Experimental Pathology, Pittsburgh Liver Research Center, University of Pittsburgh Medical Center, Division of Experimental Pathology, Department of Pathology, and Division of Gastroenterology, Hepatology and Nutrition, Department of Medicine, University of Pittsburgh School of Medicine, 200 Lothrop Street S-422 BST, Pittsburgh, PA 15261, USA. Tel: (412) 648-9966; Fax: (412) 648-1916; E-mail: smonga@pitt.edu *or* Junyan Tao, Ph.D., Division of Experimental Pathology, Department of Pathology, University of Pittsburgh School of Medicine, 200 Lothrop Street, Room S432-BST, Pittsburgh, PA 15261, USA. Tel: (412) 383-7821; Fax: (412) 648-1916; E-mail: junyantao2010@gmail.com

improved therapies[6]. Overall, there is an urgent need to actively seek new therapeutic modalities in the systemic treatment of advanced HCC[7].

The oncoproteins c-MET and β-catenin play critical roles in hepatocarcinogenesis. Overexpression of c-MET occurs in about 50% of HCC specimens[8], and about 40% of HCC tissues contain aberrant activation of β-catenin mainly due to missense mutations in the β-catenin gene[9]. In a previous study, we showed that coactivation or overexpression of c-MET and β-catenin gene mutations occurs in 9%–12.5% of all HCC patients[10]. When c-MET and mutant β-catenin were coexpressed in the liver using sleeping beauty transposon/transposase (SB) and hydrodynamic tail vein injection (HTVI), it led to occurrence of HCC with high penetrance[10]. The tumors occurring in the Met-β-catenin model displayed around 70% similarity in gene expression to clinical HCC that displayed concomitant CTNNB1 mutations and c-MET overexpression[10]. Thus, this model recapitulates around 11% of a clinical subset of HCC with high concordance and can be used to interrogate therapies for their effectiveness.

c-MET has emerged as a promising target in the development of anticancer therapeutics because of its low level of expression in normal tissues and its aberrant activation in many human cancers[11]. Several strategies have been used to inhibit c-MET activity, including c-MET- or hepatocyte growth factor (HGF)-specific antibodies or small-molecule inhibitors. In the generation of small-molecule inhibitors targeting the adenosine triphosphate (ATP)-binding pockets of the c-MET protein kinase, a major obstacle has been the high degree of sequence identity within the ATP-binding clefts of other canonical protein kinases[12]. Indeed, all currently approved small-molecule protein kinase inhibitors exhibit promiscuous binding, targeting multiple enzymes. EMD1214063, also known as tepotinib and MSC2156119, is a highly selective inhibitor of c-MET tyrosine kinase with potential antineoplastic activity[13,14]. In the current study, we investigate the antitumor efficacy of EMD1214063 in the clinically relevant Met-β-catenin mouse model to evaluate the possibility of monotherapy in HCC patients in this HCC subtype.

MATERIALS AND METHODS

Drugs

EMD1214063 [3-(1-(3-(5-(1-methylpiperidin-4-ylmethoxy)-pyrimidin-2-yl)-benzyl)-1,6-dihydro-6-oxo-pyridazin-3-yl)-benzonitrile] was obtained from Medchem Express (Cat. No. HY-14721), diluted in 5% dimethyl sulfoxide (DMSO)+corn oil and stored in aliquots at −20°C.

Animal Experiment

Wild-type FVB/N mice were obtained from the Jackson Laboratory (Bar Harbor, ME, USA). SB plasmids and HTVI have been described previously[10,15]. Briefly, 5 μg of pT3-EF5-cMET-V5 and 5 μg of pT3-EF5-S45Y-β-catenin-Myc combination along with the transposase in a ratio of 25:1 were diluted in 2 ml of normal saline (0.9% NaCl; endotoxin free; TEKnova), filtered through a 0.22-μm filter (Millipore), and injected into the lateral tail vein of 12 FVB mice that were around 6–8 weeks old in 5–7 s. These mice are referred henceforth as Met-β-catenin mice. Five weeks after injection, Met-β-catenin mice were randomized into two groups: a 5-day-on/2-day-off treatment schedule with vehicle ($n=6$, 5% DMSO plus corn oil, once a day) and EMD1214063 ($n=6$, 10 mg/kg, gavage with feeding needle, dissolved with 5% DMSO+corn oil, 0.05 mg/ml, once a day). Animals on EMD1214063 treatment were sacrificed at 8 or 11 weeks. Similarly, animals on vehicle control treatment were sacrificed at either 8 or 11 weeks.

A list of all mice used in the study is provided in Table 1. Mice were housed, fed, and monitored in accordance

Table 1. Information on all Mice Used in the Current Study

No.	Sex	Strain	Treatment	Treatment Time Point (Weeks)	Body Weight (BW) (g)	Liver Weight (LW) (g)	LW/BW×100 (%)
1	Male	FVB	Control	–	29.96	1.71	5.70
2	Male	FVB	Control	–	31.37	5.75	18.33
3	Male	FVB	Control	–	30.42	3.45	11.34
4	Male	FVB	Control	–	29.87	3.11	10.41
5	Male	FVB	Control	–	35.05	3.31	9.44
6	Male	FVB	Control	–	32.87	6.37	19.38
7	Male	FVB	EMD1214063	8	30.84	1.37	4.44
8	Male	FVB	EMD1214063	8	30.23	2.04	6.75
9	Male	FVB	EMD1214063	8	30.47	2.17	7.12
10	Male	FVB	EMD1214063	11	29.07	2.97	10.22
11	Male	FVB	EMD1214063	11	32.14	6.13	19.07
12	Male	FVB	EMD1214063	11	30.32	3.93	12.96

with the protocols approved by the Institutional Animal Care and Use Committee at the University of Pittsburgh, School of Medicine. Body weights (BWs) and liver weights (LWs) were recorded and are included in Table 1.

Immunohistochemistry

Liver specimens were fixed in 10% buffered formalin and embedded in paraffin. Hematoxylin and eosin (H&E) staining on 4-μm liver sections was performed to note the appearance and characteristics of preneoplastic and neoplastic foci at different times after tail vein injection. Immunohistochemistry (IHC) was performed on these sections as well. Briefly, deparaffinized sections were incubated in 3% H_2O_2 dissolved in 1× phosphate-buffered saline (PBS) for 30 min to quench the endogenous peroxidase. For antigen retrieval, slides were microwaved in 10 mM citrate buffer (pH 6.0) for 12 min. Subsequently, slides were incubated with primary antibodies overnight at 4°C. All the primary antibodies used in the present study are listed in Table 2. After washes, the sections were incubated in the appropriate biotin-conjugated secondary antibody (Chemicon, Temecula, CA, USA) for 30 min at room temperature. Signal was detected using the Vectastain ABC Elite Kit (Vector Laboratories, Inc., Burlingame, CA USA) and developed using diaminobenzidine (DAB; Vector Laboratories). Sections were counterstained with Shandon hematoxylin solution (Thermo Fisher Scientific, Pittsburgh, PA, USA) and passed through the dehydration process and coverslipped. For negative control, the sections were incubated with secondary antibodies only or with control immunoglobulin G (IgG).

For Sirius Red staining, samples were deparaffinized and incubated for 1 h in PicroSirius Red stain (STPSRPT; American MasterTech), washed twice in 0.5% acetic acid water, dehydrated to xylene, and coverslipped. Images were taken on an Axioskop 40 (Zeiss) inverted brightfield microscope.

All indicators were quantified by counting respective cells and total number of cells in five fields (×200 or ×50) randomly selected in each slide, and the average proportion/area of positive cells in each field was counted using the true color multifunction cell image analysis management system (Image-Pro Plus; Media Cybernetics, Bethesda, MD, USA).

TUNEL Assay

The ApopTag Plus Kit (Millipore Corp.) was employed for the TUNEL assay according to the manufacturer's instructions. Briefly, 5-μm paraffin-embedded sections were dewaxed and pretreated in 20 mg/ml proteinase K for 15 min at 37°C. Subsequently, the sections were quenched in 3% H_2O_2 at room temperature for 15 min and treated with terminal deoxynucleotidyl transferase (TdT) enzyme. The reaction was stopped by immersion in the stop/wash buffer for 15 min followed by PBS rinse for 10 min. The sections were subsequently incubated in anti-digoxigenin-peroxidase at room temperature for 30 min in a humidified chamber. After sufficient washing with PBS, the sections were visualized with DAB. Negative controls were incubated in medium lacking TdT enzyme. Nuclear immunoreactivity was considered positive. The apoptosis index corresponded to the TUNEL-labeled cells among at least 500 cells per region and was expressed as a percentage.

Western Blot Analysis

Livers from age-matched control FVB mice or various treatment groups were used to prepare whole-cell lysates as described elsewhere[10,15]. Briefly, a portion of liver was homogenized in lysis buffer [30 mM Tris (pH 7.5), 150 mM NaCl, 1% NP-40, 0.5% Na deoxycholate, 0.1% SDS, 10% glycerol, and 2 mM EDTA] containing the Complete Protease Inhibitor Cocktail (Roche Molecular Biochemicals). Protein concentrations were determined with the Bio-Rad Protein Assay Kit (Bio-Rad, Hercules, CA, USA) using bovine serum albumin (BSA) as a standard. Aliquots of 20–50 μg lysates were denatured by boiling in Tris-Glycine SDS Sample Buffer (Life Technologies, Carlsbad, CA, USA), resolved by SDS-PAGE, and transferred to polyvinylidene fluoride (PVDF) membranes (Life Technologies) using the Bio-Rad transfer apparatus (Bio-Rad). Membranes were blocked in

Table 2. Information on Antibodies Used for Immunohistochemistry in the Current Study

Antibody	Catalog No.	Company	Species	Dilution
Ki-67	NM-sP6	Thermo Scientific	Rabbit	1:100
PCNA	Sc-56	Santa Cruz Biotechnology	Mouse	1:200
TUNEL (Kit)	S7100	EMD-Millipore	NA	NA
V5-tag	14-6796-82	eBioscience	Mouse	1:50
Myc-tag	sc-788	Santa Cruz Biotechnology	Rabbit	1:200
Cyclin D1	Rb-9041-P	Thermo Scientific	Rabbit	1:200
Glutamine synthetase	Sc-74430	Santa Cruz Biotechnology	Mouse	1:100
CD45	Sc-53665	Santa Cruz Biotechnology	Mouse	1:100
α-Fetoprotein	Ab46799	Abcam	Rabbit	1:100

5% nonfat dry milk or 5% BSA in Tris-buffered saline containing 0.1% Tween 20 for 1 h and probed with various antibodies shown in Table 3. Incubation with anti-rabbit or anti-mouse secondary antibody horseradish peroxidase-conjugated IgG (Santa Cruz Biotechnology, Santa Cruz, CA, USA) was done for 30 min at room temperature. Immunoreactive bands were detected by SuperSignal West Pico Chemiluminescense Substrate or SuperSignal™ West Femto Maximum Sensitivity Substrate (Thermo Fisher Scientific, Rockford, IL, USA) and revealed by autoradiography.

Statistical Analysis

All data are presented as mean ± standard deviation (SD). All statistics were performed using Prism 6, version 6.0 (GraphPad Software Inc., La Jolla, CA, USA). The comparison between treatment and control group was performed by the Student's *t*-test. A value of $p < 0.05$ was considered significant, $p < 0.01$ was considered highly significant, and $p < 0.001$ was considered extremely significant.

RESULTS

Effect of EMD1214063 on Survival and Tumor Growth in the Met-β-Catenin HCC Model

As outlined in Materials and Methods, 8 or 11 weeks after EMD1214063 or vehicle control treatment, MET-β-catenin mice were euthanized and livers were harvested (Fig. 1A). Representative gross liver images show mostly comparable gross pathology in the form of nodularity in the control and EMD1214063 groups, although at the 8-week treatment stage the experimental group showed a decrease in gross macroscopic nodules (Fig. 1B). Although LW/BW ratio was marginally lower in the EMD1214063 group compared to the control group after 8 weeks of treatment (Table 1), the difference was not statistically significant overall or at the two individual time points ($p = 0.4659$; $p = 0.2685$; $p = 0.8184$) (Fig. 1C). Kaplan–Meier survival curve showed that treatment of Met-β-catenin model with EMD1241063 significantly improved the overall survival ($p = 0.0396$), although only marginally by 1.5–2 weeks compared to the group treated with control (Fig. 1D). This was based on time to morbidity with speculation that greater than 3 g of LW will lead to mortality. H&E staining of representative liver sections from the control group and the EMD1214063 group showed the presence of several HCC foci with basophilic cytoplasm and nuclear atypia compressing the interspersed normal eosinophilic hepatocytes in both groups and at both times, although the microscopic foci in the EMD1214063 group at 8 weeks were smaller (Fig. 1E).

To further address the overall impact of EMD121 4063 on tumor burden, we next stained for Myc-tag and V5-tag, which represent mutant β-catenin and MET-transfected hepatocytes, respectively. As expected, tumors were strongly positive for both Myc-tag as well as V5-tag in the control group at both 8 and 11 weeks (Fig. 2A). EMD1214063 treatment did not have any effect on the overall positivity for Myc-tag at both time points, and the tumor nodules continued to be present and positive for this marker (Fig. 2A). Quantification of IHC verified lack of any significant differences in the Myc-tag (Fig. 2B). Furthermore, we used whole-liver lysates from the control and experimental groups to assess overall Myc-tag levels. There was overall some decrease in Myc-tag in the EMD1214063 group at 8 weeks compared to all other times (Fig. 2C). Lack of decrease in staining for Myc-tag within tumor nodules but a modest decrease in its levels by Western blot analysis is likely due to a transiently lower tumor burden seen as smaller microscopic foci at 8 weeks of EMD1214063 treatment.

V5-tag representing c-MET-transfected cells did show a discernible decrease in the overall intensity of immunostaining albeit only at 8 weeks while tumor nodules continued to be positive for it at the 11-week time point

Table 3. Information on Antibodies Used for Western Blots in the Current Study

Antibody	Catalogue No.	Company	Species	Dilution
GAPDH	Sc-25778	Santa Cruz	Mouse	1:2,000
Myc-tag	Cs-2276s	Cell Signaling	Mouse	1:500
Cyclin D1	RB-9041-p	Thermo Scientific	Rabbit	1:1,000
AKT	Cs-4685s	Cell Signaling	Rabbit	1:1,000
p-AKT(ser473)	Cs-4060s	Cell Signaling	Rabbit	1:1,000
Glutamine synthetase	Sc-74430	Santa Cruz	Mouse	1:2,000
ERK	Cs-4695s	Cell Signaling	Rabbit	1:2,000
p-ERK (Thr202/Tyr204)	Cs-4370s	Cell Signaling	Rabbit	1:1,000
Met	Cs-3127s	Cell Signaling	Mouse	1:500
p-Met (Tyr1234/1235)	Cs-3129s	Cell Signaling	Rabbit	1:500
Stat3	Sc-8019	Santa Cruz	Mouse	1:500
p-Stat3 (Tyr705)	Cs-9131	Cell Signaling	Rabbit	1:1,000

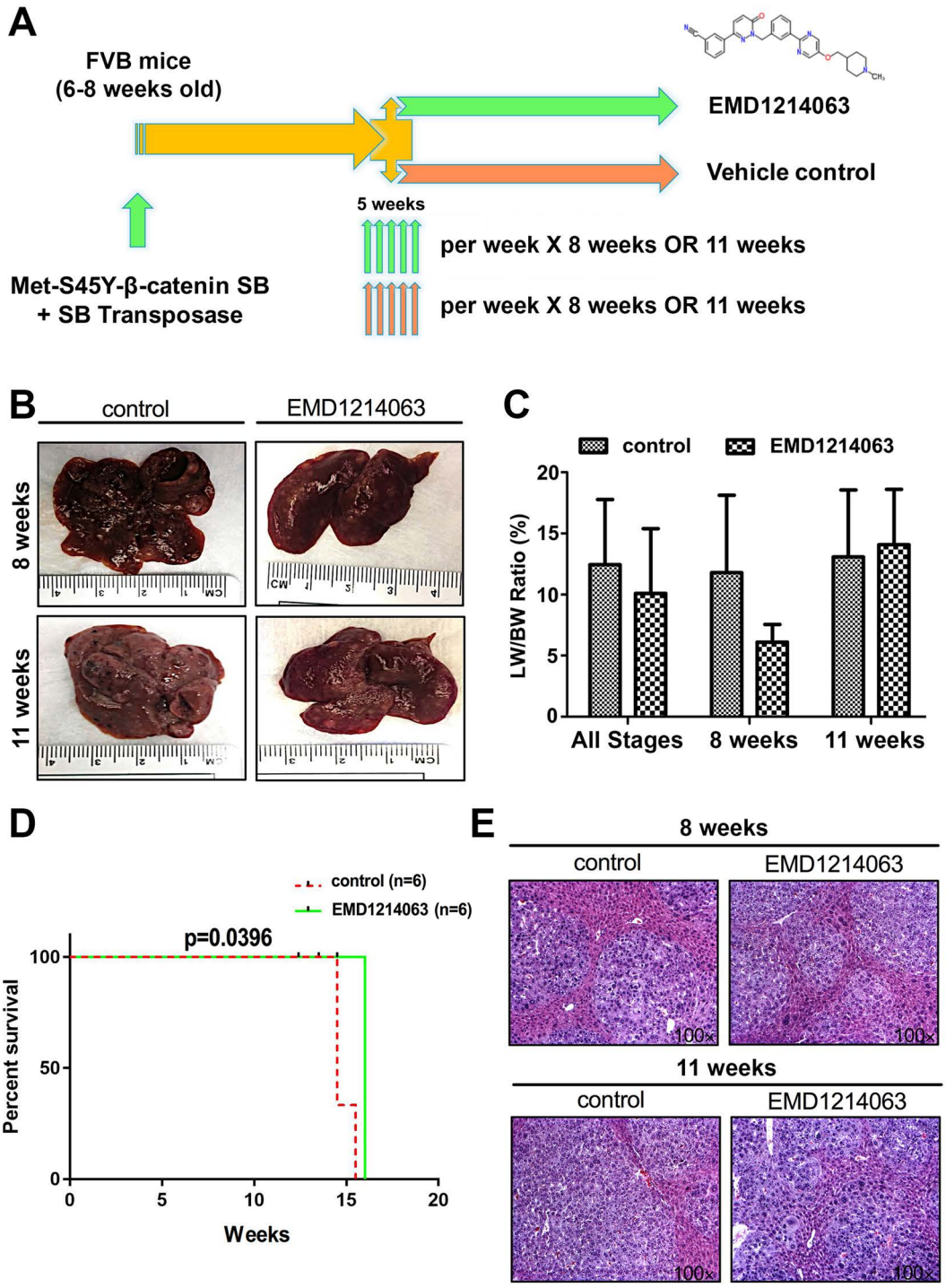

Figure 1. A marginal improvement in overall survival but lack of any significant effect of treatment with the c-MET inhibitor EMD1214063 for 8 or 11 weeks on tumor growth in the Met-β-catenin model. (A) Schematic illustrating the overall experimental design of the study. (B) Gross liver images show comparable morphology between the control and EMD1241063 groups, although this group showed a somewhat healthy appearance at 8 weeks as shown by lack of relative nodularity. (C) No significant difference in liver weight/body weight (LW/BW) ratio as an indicator of overall tumor burden between the control and EMD1214063 treatment groups overall or at 8 or 11 weeks individually [average ± standard deviation (SD)]. (D) Kaplan–Meier survival curve showing EMD1241063 treatment causing marginal but significant improvement in the overall survival by 1.5–2 weeks compared to the control treatment in the Met-β-catenin model ($p = 0.0396$). This was based on time to morbidity as indicated by greater than 3 g of liver weight due to excessive tumor burden. (E) Hematoxylin and eosin (H&E) staining of representative liver sections from the EMD1214063 group versus controls shows comparable microscopic foci.

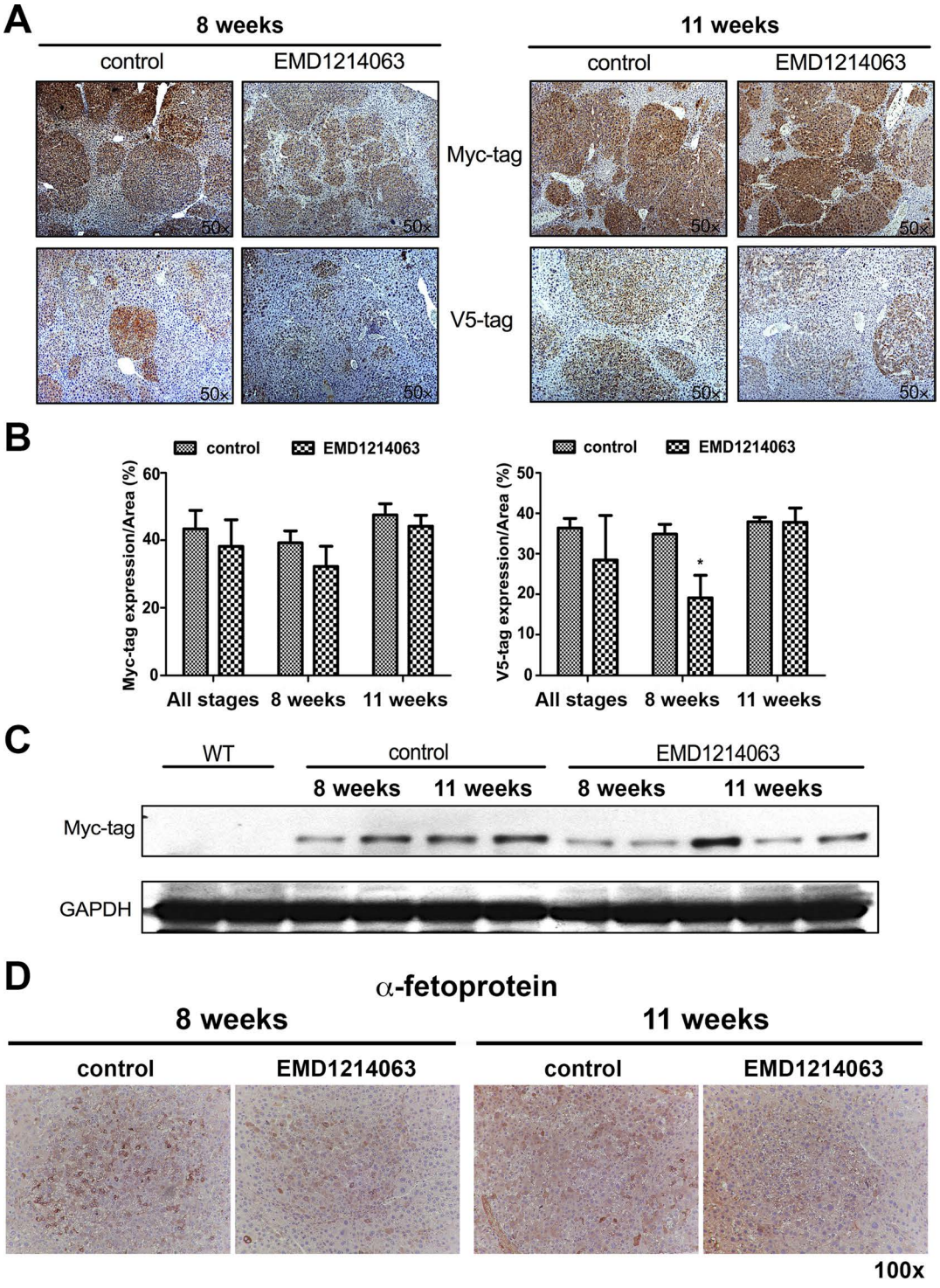

Figure 2. EMD1214063 treatment of the Met-β-catenin model temporally decreases V5-tag (c-MET) but not Myc-tag (β-catenin). (A) Microscopic foci show positivity for both Myc-tag and V5-tag in the control group at both 8 and 11 weeks. EMD1214063 treatment did not have any effect on staining for Myc-tag. Staining for V5-tag showed smaller and fainter positive tumor foci after 8 weeks of EMD1214063, but no difference was observed at 11 weeks. (B) Quantification of immunohistochemistry (IHC) verified lack of significant differences in Myc-tag but showed a significant decrease in V5-tag staining (*$p = 0.0465$) after EMD1214063 treatment for 8 weeks only. (C) Western blot for Myc-tag showed decrease in Myc-tag levels at 8 weeks of EMD1214063 treatment only. GAPDH shows comparable loading in all lanes. (D) IHC for α-fetoprotein shows tumors to be positive in both control- and EMD1214063-treated group at both 8 and 11 weeks.

(Fig. 2A). Quantification of IHC verified a significant decrease in V5-tag staining in EMD1214063 treatment versus the controls ($p=0.0465$) at 8 weeks, indicating the short-term advantage of c-MET inhibition in the Met-β-catenin model (Fig. 2B).

We next examined HCCs in the Met-β-catenin model for expression of α-fetoprotein, a common oncofetal marker upregulated in the majority of these tumors. Indeed, Met-β-catenin HCCs were positive for α-fetoprotein at both time points examined, although there was intratumoral heterogeneity in its expression (Fig. 2C). Treatment with 8 or 11 weeks of EMD1214063 did not have an impact on overall α-fetoprotein expression in HCCs compared to controls (Fig. 2C).

Thus, overall the microscopic and macroscopic tumor burden appeared comparable in both the control and experimental groups, especially at the longer time point.

Effect of EMD1214063 on β-Catenin Activation in the Met-β-Catenin HCC Model

To address the effect of the MET inhibitor EMD 1214063 on Wnt signaling, we performed IHC for key β-catenin target glutamine synthetase (GS). GS is a downstream target of β-catenin and has been shown to be a reliable biomarker of stabilizing mutations in CTNNB1[16–18]. We did not find any difference in the staining intensity for GS in the experimental versus control group at 8 or 11 weeks (Fig. 3A). The quantification of IHC for GS verified lack of any difference between the EMD1214063 and controls (Fig. 3B). Interestingly, like Western blot analysis for Myc-tag, we observed a marginal decrease in GS levels at 8 weeks in the EMD1214063 treatment group, while comparable levels were evident at 11 weeks (Fig. 3C). Taken together, it is likely that transient decrease in GS levels at 8 weeks is reflective of marginally lesser tumor burden as reflected by smaller microscopic tumor foci after the EMD1214063 treatment.

EMD1214063 Inhibits the c-MET Pathway in the Met-β-Catenin HCC Model

To specifically address the efficacy of EMD1214063 in blocking c-MET signaling and determine effects on its downstream signaling, we used tumor-bearing livers from 8- to 11-week control or EMD1214063 treatment groups for Western blot analysis. A modest decrease in p-c-MET (Tyr1234/1235) levels was evident in the EMD1214063-treated group compared to the controls, while total c-MET levels remained unaffected (Fig. 4). The overall effect on p-c-MET was more prominent at 11 weeks. Since c-MET activation can lead to diverse downstream signaling, we next assessed AKT, ERK, and STAT signaling, which represent distinct signaling arms[19]. Compared to WT livers,

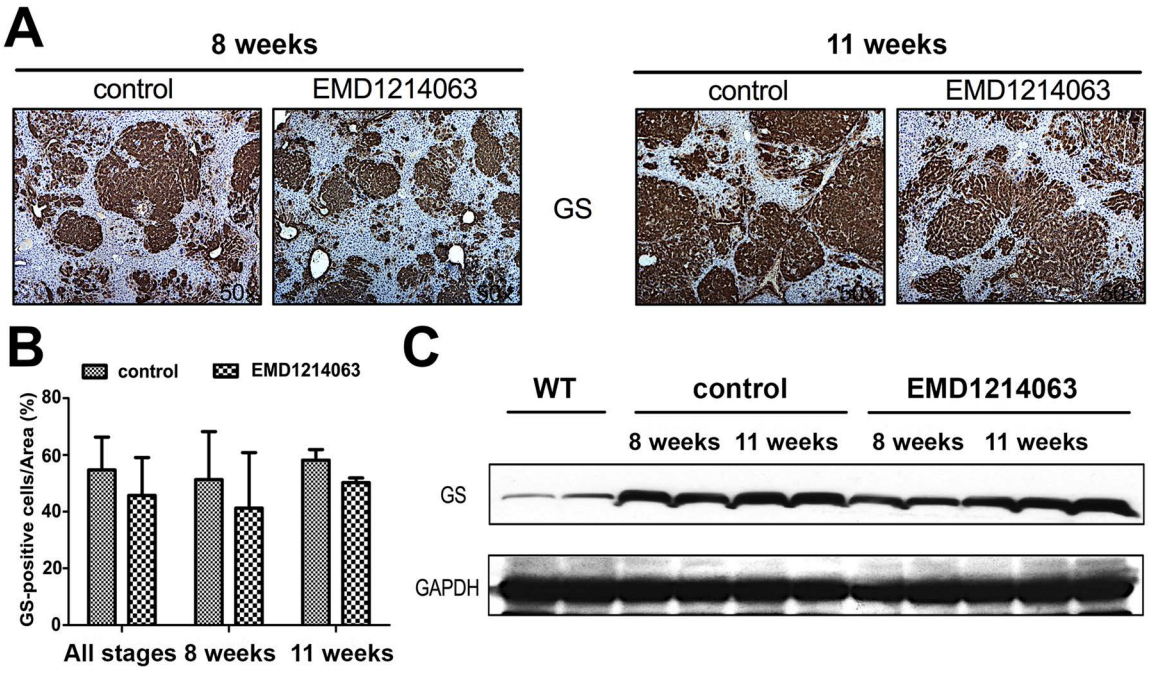

Figure 3. EMD1214063 does not impact β-catenin signaling in the Met-β-catenin model. (A) Microscopic foci show positivity for glutamine synthetase (GS) in the control- and EMD1214063-treated groups at both 8 and 11 weeks. (B) Quantification of immunostaining showed lack of any differences in the control and experimental group at either or both time points after EMD1214063 treatment. (C) EMD1214063 treatment showed a marginal decrease in total GS levels by Western blot analysis at only 8 weeks. GAPDH shows comparable loading in all lanes.

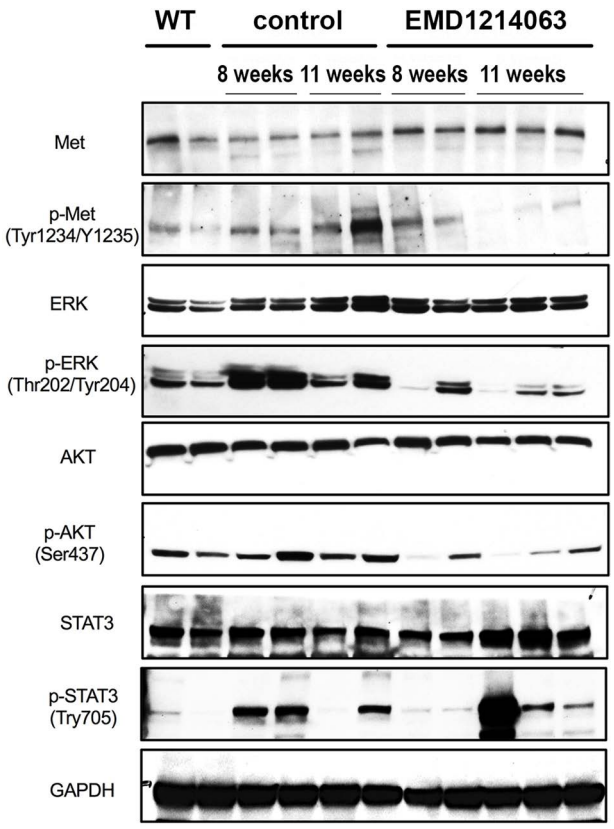

Figure 4. EMD1214063 inhibits c-MET signaling in the Met-β-catenin hepatocellular carcinoma (HCC) mouse model. Western blot analysis using whole-liver lysates from control- and EMD1214063-treated groups at 8 and 11 weeks shows a notable decrease in the levels of p-Met (Tyr1234/1235), p-ERK1/2 (Thr202/Tyr204), p-AKT (Ser473), and p-STAT3 (Tyr705) levels in the EMD1214063-treated group. GAPDH shows comparable loading in all lanes.

Met-β-catenin livers showed increased levels of p-AKT, p-ERK, and p-STAT3, as also reported previously[10]. Compared to the control, treatment with EMD1214063 led to notable decreases in p-AKT (Ser473), p-ERK (Thr202/Tyr204), and p-STAT3 (Tyr705) levels at both 8 weeks and 11 weeks (Fig. 4). These results suggest EMD1214063 effectively suppresses c-MET signaling to inhibit ERK, phosphoinositide 3-kinase/AKT, and JAK/STAT signaling in the Met-β-catenin HCC mouse model even though only marginal biological response in the form of lower tumor burden was evident transiently at 8 weeks.

Effect of EMD1214063 on Tumor Cell Survival and Proliferation in the Met-β-Catenin Model

Since EMD1214063 predictably had no effect on β-catenin signaling but impacted c-MET signaling while temporally and transiently lowering tumor burden at 8 weeks of treatment and improving survival marginally but significantly, we next interrogated the basis of this effect. The effect of EMD1214063 on cell viability and proliferation in the Met-β-catenin model was examined by IHC for TUNEL, and Ki-67, PCNA, and cyclin D1, respectively. TUNEL staining showed a few apoptotic nuclei in both groups at both time points (Fig. 5A), and its quantification revealed insignificant differences (Fig. 5B). The numbers of Ki-67$^+$ cells were significantly lower in the tumors from the EMD1214063 group compared to those from the control group in combined analysis from 8 to 11 weeks ($p=0.0004$), at 8 weeks ($p=0.0096$), and at 11 weeks ($p=0.042$) (Fig. 5A and B). Likewise, numbers of PCNA$^+$ cells were significantly lower in the tumors in the EMD1214063 treatment group compared to controls in the combined analysis from 8 to 11 weeks ($p=0.0016$) and at 8 weeks ($p=0.0225$) (Fig. 5A and B).

Cyclin D1 is a member of the cyclin protein family that is involved in regulating cell cycle progression. The number of cyclin D1$^+$ cells was significantly lower in the tumors from the EMD1214063 group compared to those from the control group (Fig. 5A), at all stages combined ($p<0.0001$), at 8 weeks ($p=0.0330$), and at 11 weeks ($p=0.0028$) (Fig. 5C). Western blot analysis similarly confirmed a modest and consistent decrease in cyclin D1 levels in the EMD1214063 group versus controls, verifying that suppression of c-MET reduced the protein levels of proproliferative cyclin D1 (Fig. 5D).

Thus, inhibition of c-MET signaling in the Met-β-catenin model affected tumor burden and overall survival marginally, likely due to its effect on tumor cell proliferation.

FACING PAGE

Figure 5. EMD1214063 reduces cell proliferation after 8 and 11 weeks of treatment of Met-β-catenin mice, which is associated with a decrease in cyclin D1 levels. (A) IHC for Ki-67 and PCNA shows decrease in the EMD1214063 treatment group compared with the control group at both 8 and 11 weeks after treatment. Cyclin D1 levels were also reduced. No change in the number of TUNEL$^+$ cells was evident after EMD1214063 treatment at either time point. (B) Quantification of TUNEL, Ki-67, and PCNA immunohistochemistry shows insignificant difference in apoptosis, but significant differences in Ki-67 at combined time points (***$p=0.0004$), at 8 weeks (**$p=0.0096$), and at 11 weeks (*$p=0.042$), as well as PCNA at combined time points (**$p=0.0016$) or at 8 weeks (*$p=0.0225$). (C) Quantification of cyclin D1 staining showed a significant difference in EMD1214063-treated samples compared to controls at both times combined (***$p<0.0001$), at 8 weeks (*$p=0.0330$), and at 11 weeks (**$p=0.0028$). (D) Decrease in levels of cyclin D1 after EMD1214063 was verified by Western blots as well. GAPDH shows comparable loading in all lanes.

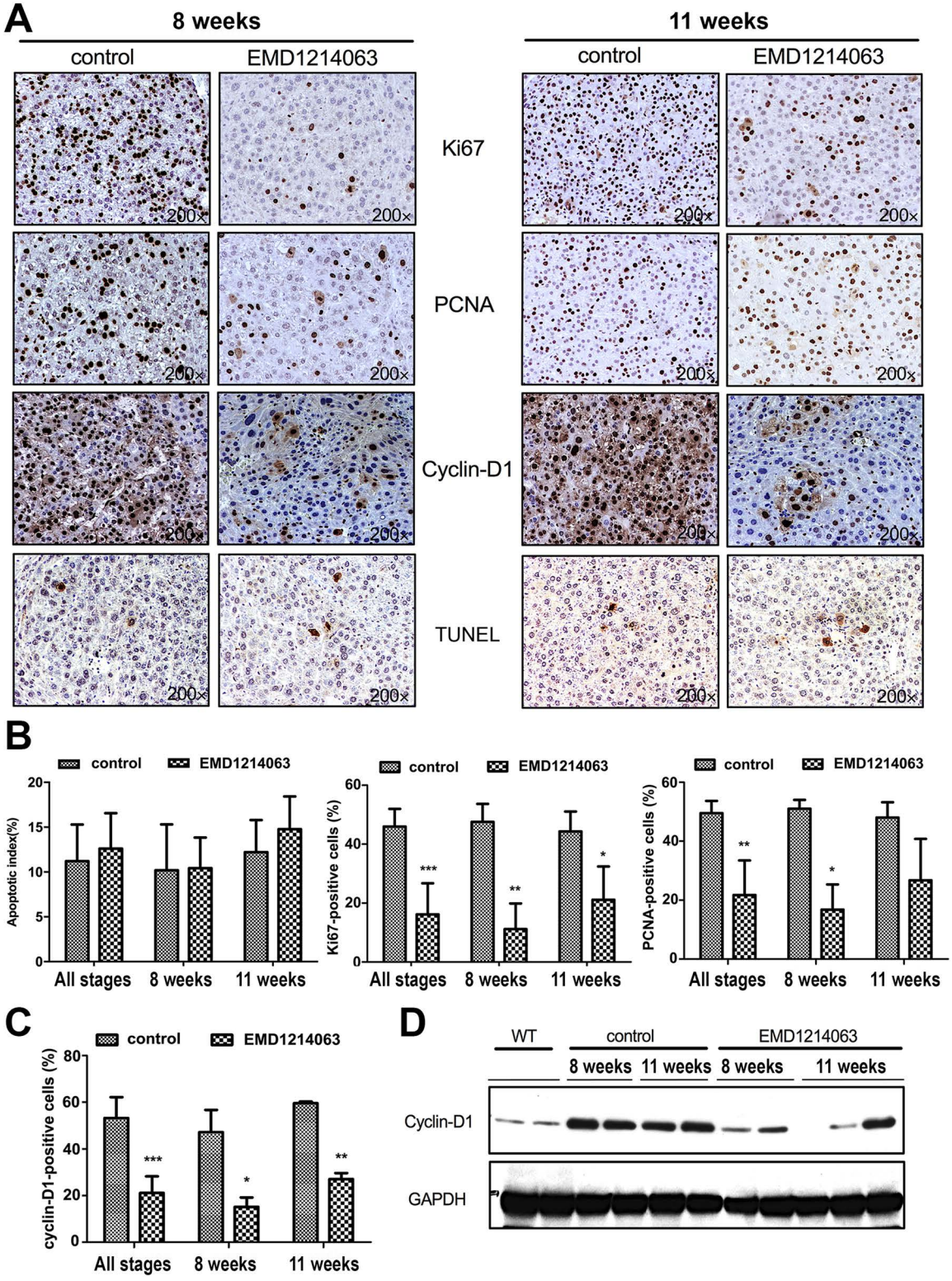
A
8 weeks
11 weeks
control
EMD1214063
control
EMD1214063
Ki67
PCNA
Cyclin-D1
TUNEL
200×
B
control
EMD1214063
Apoptotic index(%)
All stages
8 weeks
11 weeks
Ki67-positive cells (%)
PCNA-positive cells (%)
C
cyclin-D1-positive cells (%)
D
WT
control
EMD1214063
8 weeks
11 weeks
8 weeks
11 weeks
Cyclin-D1
GAPDH

Effect of EMD1214063 on Inflammation and Fibrosis in the Met-β-Catenin Model

Last, we wanted to address if Met inhibition had any effect on overall inflammation in the Met-β-catenin HCC model. We assessed livers from controls and the EMD1214063-treated group at 8 and 11 weeks for $CD45^+$ cells. $CD45^+$ inflammatory cells were present both outside and within the tumor nodules at both 8 and 11 weeks in control, which remained unchanged in the corresponding EMD1214063-treated groups (Fig. 6A).

To address if there was any evidence of ongoing fibrosis in the Met-β-catenin model, we first assessed livers from 8- to 11-week control-treated mice for Sirius Red staining. As expected, staining for Sirius Red was evident around vascular structures in the liver section, but otherwise minimal to no positivity for this stain for collagen was evident within or outside the tumors in the controls (Fig. 6B). Likewise, there was no change in staining after 8 or 11 weeks of treatment with EMD1214063 (Fig. 6B).

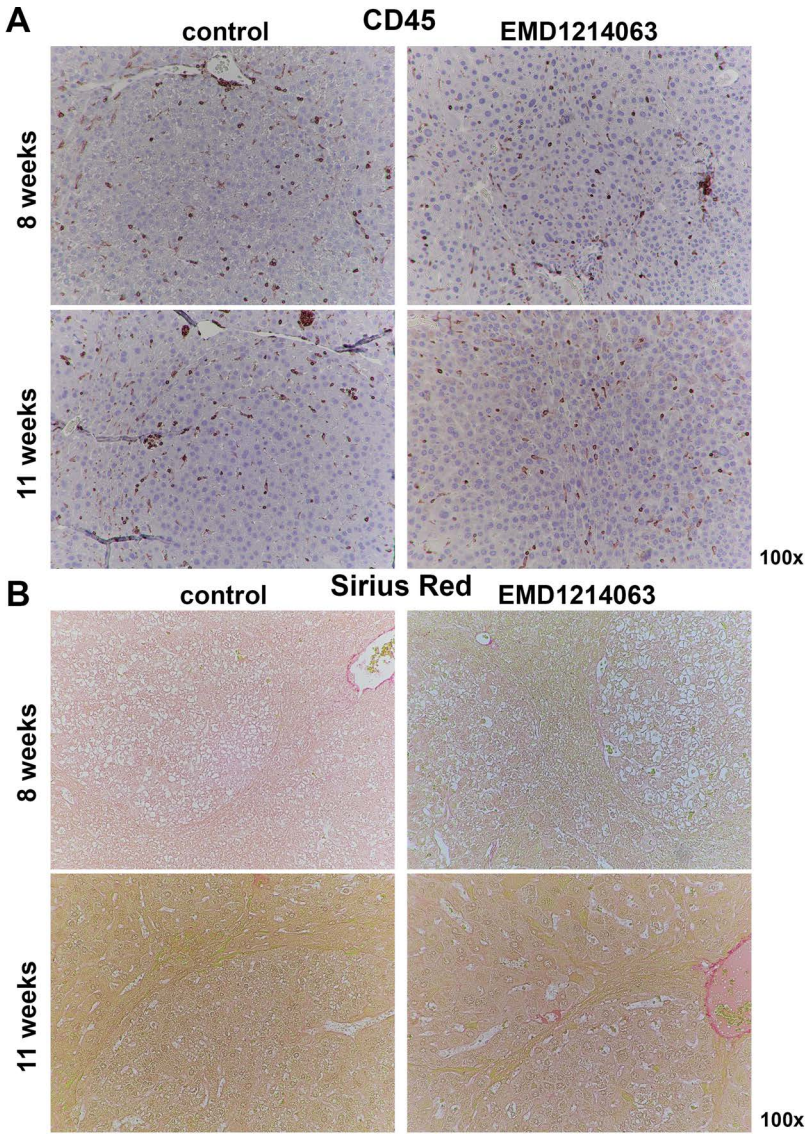

Figure 6. EMD1214063 does not impact inflammation or fibrosis at 8 weeks or 11 weeks of treatment of Met-β-catenin mice. (A) IHC for CD45 shows comparable inflammatory cells both within and outside the tumor foci at 8 weeks or 11 weeks in controls or EMD1214063 treatment group. (B) Sirius Red staining shows lack of any hepatic fibrosis in control-treated Met-β-catenin mice at either 8 or 11 weeks. No differences between controls and EMD1214063 treatment were evident at either time points.

Thus, c-Met inhibition did not impact overall inflammation or fibrosis in the Met-β-catenin HCC model.

DISCUSSION

Our previous studies found 9%–12.5% of HCC patients have β-catenin mutations and c-MET activation[10]. Using a reductionist approach, we coexpressed c-MET and mutant β-catenin, which led to HCC that showed high concordance to a subset of human HCC, and the tumors displayed activation of c-MET and β-catenin. This model allows us a unique opportunity to study the biology of this subset of tumors and allows us to evaluate novel therapies as a step toward precision medicine[10].

Previously, we showed that downstream of c-MET, Ras activation was important in HCC pathogenesis. In fact, when c-MET was replaced by mutant KRAS and coexpressed with mutant β-catenin using the SB-HTVI, it led to HCC that was more than 90% similar to Met-β-catenin HCC by gene expression studies[15]. Further, we showed that HCC in this model was highly responsive to β-catenin suppression, suggesting that these tumors are dependent on Wnt signaling for their growth and development[15].

Here we wanted to directly address the relevance of c-MET suppression as a therapeutic strategy for this HCC subset. The role of c-MET in HCC is unquestionable[19]. Its role in the different stages of HCC is also well described[8]. c-MET activity has also been shown to confer resistance to sorafenib therapy in HCC[20]. Although inhibitors of c-MET/HGF signaling have demonstrated antitumor potential in preclinical HCC models by decreasing hepatocellular tumor cell proliferation, cell motility, and invasion, and promoting apoptosis[21], whether this strategy will be beneficial in a clinical subset where c-MET and β-catenin cooperate in HCC development and growth remains elusive and was the topic of our investigation. We used EMD1214063 to test its efficacy in the Met-β-catenin-driven HCC model.

EMD1214063, also known as tepotinib or MSC21 56119, is a highly selective inhibitor of c-MET tyrosine kinase with potential antineoplastic activity and has also shown signs of efficacy in the treatment of HCC, particularly against c-MET$^+$ tumors in vivo[13,14] and in clinical trials[22].

Our studies intriguingly showed only a modest overall effect on HCC in the Met-β-catenin model as seen by a transient decrease in overall tumor burden at 8 weeks after treatment and a marginal but significant improvement in overall survival. No effect on Wnt signaling was evident, but c-MET signaling was affected, which was seen by a decrease in V5-tag in EMD1214063 versus controls at earlier treatment stage. We did observe a notable decrease in p-MET levels with EMD1214063 treatment, which impacted downstream signaling, especially mitogen-activated protein kinase kinase/ERK, phosphoinositide 3-kinase/AKT, and STAT3[11,19,21]. The ultimate effect of c-MET suppression on tumor biology was not due to the effect on tumor cell survival. We did not observe any effect on inflammation within the tumor foci and outside after EMD1214063 treatment. Tumors also continued to be α-fetoprotein$^+$ in both groups. EMD1214063 treatment did suppress cell proliferation, albeit modestly and temporally, likely through affecting cyclin D1 levels.

Cyclin D1 belongs to the D-type cyclin family and interacts with cyclin-dependent kinase (Cdk) 4/6, which in turn phosphorylates the retinoblastoma (Rb) protein, thereby promoting the transition from the G_1 to S phase of the cell cycle[23,24]. Cyclin D1 overexpression can play a multitude of roles in tumors, including contributing to cell proliferation, cell survival, chromosomal instability, restraint of autophagy, and potentially through other noncanonical functions[23,25–29]. Decrease in cyclin D1 that was apparent after EMD1214063 treatment was associated with lower cell proliferation. This was intriguing because cyclin D1 can be under β-catenin signaling control, especially in the liver in both regeneration and in cancer[30–32].

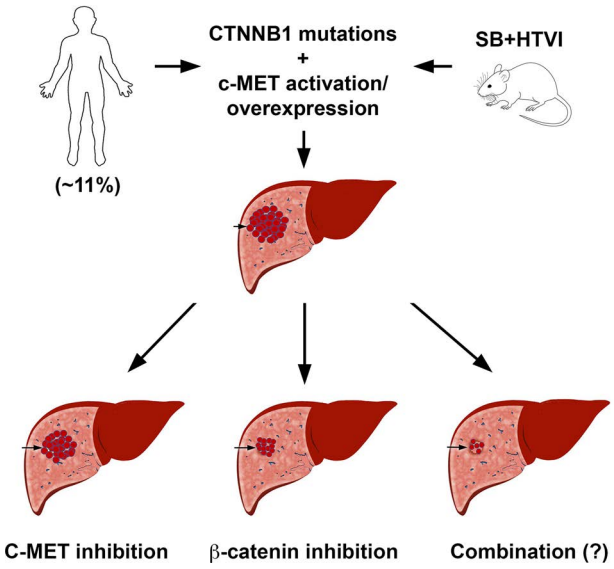

Figure 7. Cartoon depicting relative response of HCC in the Met-β-catenin mice to c-MET or β-catenin suppression. Eleven percent of all human HCCs shows concomitant β-catenin mutations and c-MET overexpression or activation. Coexpression of these two proto-oncogenes in mouse liver leads to HCC, which molecularly resembles the subset of human HCC with simultaneous β-catenin mutations and c-MET activation. When treated with c-MET inhibitors after tumors were established, only a marginal effect on overall HCC burden was observed. However, suppression of β-catenin led to a profound response, and tumors were notably eliminated in a predominant subset of mice. It is anticipated that HCC in this model may respond even more profoundly to combined c-MET and β-catenin suppression, although it has not been directly investigated yet.

We identified cyclin D1 decrease despite no change in β-catenin signaling downstream of c-MET inhibition. However, HGF/c-MET signaling can regulate cyclin D1 expression[33,34]. We are unsure of the precise downstream effector of c-MET signaling whose suppression by EMD1214063 treatment reduces cyclin D1.

Our study underscores the relative contribution of β-catenin signaling in tumor growth of Met-β-catenin HCCs once established. Inhibition of c-MET with EMD1214063 only had a marginal effect, whereas suppression of β-catenin in an analogous Kras-β-catenin model showed a complete response[15]. Interestingly, in another recent study from our group, we showed that a thyromimetic small molecule that activates thyroid receptor-β (GC-1) also coincidentally inhibited c-MET activation and only marginally reduced tumor growth, very similar to EMD1214063 treatment[35]. Taken together, these studies suggest that inhibiting c-MET signaling alone will not be sufficient to profoundly impact HCC in the Met-β-catenin model, which represents around 11% of all human HCCs (Fig. 7). We propose that a combination of c-MET inhibitor and β-catenin inhibitor would be a more effective therapy for HCC, which displays concomitant CTNNB1 mutations and c-MET activation.

ACKNOWLEDGMENTS: This work was supported by National Institutes of Health (NIH) grants 1R01DK62277, 1R01DK 100287, and 1R01CA204586, and Endowed Chair for Experimental Pathology (S.P.M.). The authors declare no conflicts of interest.

REFERENCES

1. El-Serag HB. Hepatocellular carcinoma. N Engl J Med. 2011;365(12):1118–27.
2. Jemal A, Bray F, Center MM, Ferlay J, Ward E, Forman D. Global cancer statistics. CA Cancer J Clin. 2011;61 (2):69–90.
3. 2017 Cancer stat facts: Liver and intrahepatic bile duct cancer. Available at https://seer.cancer.gov/statfacts/html/livibd.html
4. Golabi P, Fazel S, Otgonsuren M, Sayiner M, Locklear CT, Younossi ZM. Mortality assessment of patients with hepatocellular carcinoma according to underlying disease and treatment modalities. Medicine (Baltimore) 2017;96 (9):e5904.
5. Bruix J, Qin S, Merle P, Granito A, Huang YH, Bodoky G, Pracht M, Yokosuka O, Rosmorduc O, Breder V, Gerolami R, Masi G, Ross PJ, Song T, Bronowicki JP, Ollivier-Hourmand I, Kudo M, Cheng AL, Llovet JM, Finn RS, LeBerre MA, Baumhauer A, Meinhardt G, Han G; RESORCE Investigators. Regorafenib for patients with hepatocellular carcinoma who progressed on sorafenib treatment (RESORCE): A randomised, double-blind, placebo-controlled, phase 3 trial. Lancet 2017;389(10064): 56–66.
6. 2017 FDA grants accelerated approval to nivolumab for HCC previously treated with sorafenib. Available at https://www.fda.gov/Drugs/InformationOnDrugs/ApprovedDrugs/ucm577166.htm
7. Gong XL, Qin SK. Progress in systemic therapy of advanced hepatocellular carcinoma. World J Gastroenterol. 2016;22(29):6582–94.
8. Tward AD, Jones KD, Yant S, Cheung ST, Fan ST, Chen X, Kay MA, Wang R, Bishop JM. Distinct pathways of genomic progression to benign and malignant tumors of the liver. Proc Natl Acad Sci USA 2007;104(37):14771–6.
9. Schulze K, Imbeaud S, Letouze E, Alexandrov LB, Calderaro J, Rebouissou S, Couchy G, Meiller C, Shinde J, Soysouvanh F, Calatayud AL, Pinyol R, Pelletier L, Balabaud C, Laurent A, Blanc JF, Mazzaferro V, Calvo F, Villanueva A, Nault JC, Bioulac-Sage P, Stratton MR, Llovet JM, Zucman-Rossi1 J. Exome sequencing of hepatocellular carcinomas identifies new mutational signatures and potential therapeutic targets. Nat Genet. 2015;47(5):505–11.
10. Tao J, Xu E, Zhao Y, Singh S, Li X, Couchy G, Chen X, Zucman-Rossi J, Chikina M, Monga SP. Modeling a human hepatocellular carcinoma subset in mice through coexpression of met and point-mutant beta-catenin. Hepatology 2016;64(5):1587–605.
11. Graveel CR, Tolbert D, Vande Woude GF. MET: A critical player in tumorigenesis and therapeutic target. Cold Spring Harb Perspect Biol. 2013;5(7).
12. Buchanan SG, Hendle J, Lee PS, Smith CR, Bounaud PY, Jessen KA, Tang CM, Huser NH, Felce JD, Froning KJ, Peterman MC, Aubol BE, Gessert SF, Sauder JM, Schwinn KD, Russell M, Rooney IA, Adams J, Leon BC, Do TH, Blaney JM, Sprengeler PA, Thompson DA, Smyth L, Pelletier LA, Atwell S, Holme K, Wasserman SR, Emtage S, Burley SK, Reich SH. SGX523 is an exquisitely selective, ATP-competitive inhibitor of the MET receptor tyrosine kinase with antitumor activity in vivo. Mol Cancer Ther. 2009;8(12):3181–90.
13. Bladt F, Faden B, Friese-Hamim M, Knuehl C, Wilm C, Fittschen C, Gradler U, Meyring M, Dorsch D, Jaehrling F, Pehl U, Stieber F, Schadt O, Blaukat A. EMD 1214063 and EMD 1204831 constitute a new class of potent and highly selective c-Met inhibitors. Clin Cancer Res. 2013; 19(11):2941–51.
14. Bladt F, Friese-Hamim M, Ihling C, Wilm C, Blaukat A. The c-Met inhibitor MSC2156119J effectively inhibits tumor growth in liver cancer models. Cancers (Basel) 2014; 6(3):1736–52.
15. Tao J, Zhang R, Singh S, Poddar M, Xu E, Oertel M, Chen X, Ganesh S, Abrams M, Monga SP. Targeting beta-catenin in hepatocellular cancers induced by coexpression of mutant beta-catenin and K-Ras in mice. Hepatology 2017;65(5):1581–99.
16. Cadoret A, Ovejero C, Terris B, Souil E, Levy L, Lamers WH, Kitajewski J, Kahn A, Perret C. New targets of beta-catenin signaling in the liver are involved in the glutamine metabolism. Oncogene 2002;21(54):8293–301.
17. Cieply B, Zeng G, Proverbs-Singh T, Geller DA, Monga SP. Unique phenotype of hepatocellular cancers with exon-3 mutations in beta-catenin gene. Hepatology 2009; 49(3):821–31.
18. Zucman-Rossi J, Benhamouche S, Godard C, Boyault S, Grimber G, Balabaud C, Cunha AS, Bioulac-Sage P, Perret C. Differential effects of inactivated Axin1 and activated beta-catenin mutations in human hepatocellular carcinomas. Oncogene 2007;26(5):774–80.
19. Giordano S, Columbano A. Met as a therapeutic target in HCC: Facts and hopes. J Hepatol. 2014;60(2):442–52.

20. Chen J, Jin R, Zhao J, Liu J, Ying H, Yan H, Zhou S, Liang Y, Huang D, Liang X, Yu H, Lin H, Cai X. Potential molecular, cellular and microenvironmental mechanism of sorafenib resistance in hepatocellular carcinoma. Cancer Lett. 2015;367(1):1–11.
21. You H, Ding W, Dang H, Jiang Y, Rountree CB. c-Met represents a potential therapeutic target for personalized treatment in hepatocellular carcinoma. Hepatology 2011; 54(3):879–89.
22. Qin S, Lim HY, Ryoo BY, Li C, Xiong H, Ihling C, Cheng AL. 2353 Data from a phase Ib/II trial of the oral c-Met inhibitor tepotinib (MSC2156119J) as first-line therapy in Asian patients with advanced hepatocellular carcinoma. Eur J Cancer 2015;51:S452–3.
23. Ewen ME, Lamb J. The activities of cyclin D1 that drive tumorigenesis. Trends Mol Med. 2004;10(4):158–62.
24. Fu M, Wang C, Li Z, Sakamaki T, Pestell RG. Minireview: Cyclin D1: Normal and abnormal functions. Endocrinology 2004;145(12):5439–47.
25. Brown NE, Jeselsohn R, Bihani T, Hu MG, Foltopoulou P, Kuperwasser C, Hinds PW. Cyclin D1 activity regulates autophagy and senescence in the mammary epithelium. Cancer Res. 2012;72(24):6477–89.
26. Casimiro MC, Crosariol M, Loro E, Ertel A, Yu Z, Dampier W, Saria EA, Papanikolaou A, Stanek TJ, Li Z, Wang C, Fortina P, Addya S, Tozeren A, Knudsen ES, Arnold A, Pestell RG. ChIP sequencing of cyclin D1 reveals a transcriptional role in chromosomal instability in mice. J Clin Invest. 2012;122(3):833–43.
27. Casimiro MC, Di Sante G, Crosariol M, Loro E, Dampier W, Ertel A, Yu Z, Saria EA, Papanikolaou A, Li Z, Wang C, Addya S, Lisanti MP, Fortina P, Cardiff RD, Tozeren A, Knudsen ES, Arnold A, Pestell RG. Kinase-independent role of cyclin D1 in chromosomal instability and mammary tumorigenesis. Oncotarget 2015;6(11):8525–38.
28. Casimiro MC, Di Sante G, Di Rocco A, Loro E, Pupo C, Pestell TG, Bisetto S, Velasco-Velazquez MA, Jiao X, Li Z, Kusminski CM, Seifert EL, Wang C, Ly D, Zheng B, Shen CH, Scherer PE, Pestell RG. Cyclin D1 restrains oncogene-induced autophagy by regulating the AMPK-LKB1 signaling axis. Cancer Res. 2017;77(13):3391–405.
29. Pestell RG. New roles of cyclin D1. Am J Pathol. 2013;183 (1):3–9.
30. Patil MA, Lee SA, Macias E, Lam ET, Xu C, Jones KD, Ho C, Rodriguez-Puebla M, Chen X. Role of cyclin D1 as a mediator of c-Met- and beta-catenin-induced hepatocarcinogenesis. Cancer Res. 2009;69(1):253–61.
31. Tan X, Behari J, Cieply B, Michalopoulos GK, Monga SP. Conditional deletion of beta-catenin reveals its role in liver growth and regeneration. Gastroenterology 2006;131 (5):1561–72.
32. Torre C, Benhamouche S, Mitchell C, Godard C, Veber P, Letourneur F, Cagnard N, Jacques S, Finzi L, Perret C, Colnot S. The transforming growth factor-alpha and cyclin D1 genes are direct targets of beta-catenin signaling in hepatocyte proliferation. J Hepatol. 2011;55(1):86–95.
33. Li Y, Lal B, Kwon S, Fan X, Saldanha U, Reznik TE, Kuchner EB, Eberhart C, Laterra J, Abounader R. The scatter factor/hepatocyte growth factor: c-Met pathway in human embryonal central nervous system tumor malignancy. Cancer Res. 2005;65(20):9355–62.
34. Recio JA, Merlino G. Hepatocyte growth factor/scatter factor activates proliferation in melanoma cells through p38 MAPK, ATF-2 and cyclin D1. Oncogene 2002;21(7): 1000–8.
35. Puliga E, Min Q, Tao J, Zhang R, Pradhan-Sundd T, Poddar M, Singh S, Columbano A, Yu J, Monga SP. Thyroid hormone receptor-β agonist GC-1 inhibits Met-β-catenin-driven hepatocellular cancer. Am J Pathol. 2017;187(11):2473–85.